

OPENFOAM SIMULATION OF MASS TRANSFER IN SPACER-FILLED CHANNELS

José L.C. Santos^{*†}, João G. Crespo[†], Vítor Geraldes^{††}

[†]Requimte/CQFB, Departamento de Química, Faculdade de Ciências e Tecnologia,
Universidade Nova de Lisboa,
Campus de Caparica, 2829-516 Caparica, Portugal
e-mail: {jose.santos,jgc}@dq.fct.unl.pt

^{††}ICEMS, Departamento de Engenharia Química e Biológica, Instituto Superior Técnico,
Universidade Técnica de Lisboa
Av. Rovisco Pais 1, 1049-001 Lisboa, Portugal
e-mail: vitor.geraldes@ist.utl.pt

Key words: Mass transfer, Spacer, Membrane processing, Wall shear stress, High Schmidt number, OpenFOAM

Abstract. *The present work describes a numerical methodology for the simulation of flow and mass transfer in spacer-filled channels presenting high Schmidt numbers using OpenFOAM. The computational mesh was generated using blockMesh, and the solver was developed using channelFoam as a template by replacing the PISO loop by PIMPLE, and introducing the solute mass fraction equation and Sherwood number calculation. The flow field results obtained compare very well with those found in the literature using commercial CFD packages. A mass transfer correlation developed from the numerical results shows different Re and Sc dependences than recent publications. These different results may be attributed to the wider range of Sc numbers studied in this work.*

1 INTRODUCTION

The design and optimization of the operating conditions of membrane modules requires rigorous knowledge about the hydrodynamic and mass transfer in the feed channel. Net-type spacers are conventionally used in the feed channel to enhance mass transfer and minimize fouling and concentration polarization effects. CFD may be regarded as a useful tool to assist in the design of optimized spacers that enables an increase in the mass transfer performance of the membrane module without compromising its pressure drop. In a recent study¹ it has been shown that the open-source OpenFOAM CFD package could be used with high confidence in the simulation of the flow in channels filled with spacers that are aligned with the main flow direction. One of the main challenges is still the validation of a methodology able to describe mass transfer of systems exhibiting high Schmidt numbers representative of industrial applications of membrane processing, mainly due to periodicity effects and very thin concentration boundary layers observed in these systems^{2,3}. The present work describes a numerical methodology for the simulation of systems presenting high Schmidt numbers using OpenFOAM.

2 PHYSICAL AND MATHEMATICAL MODEL

The flow geometry considered in this work is representative of a spacer typically used in spiral-wound membrane modules. A spacer is comprised of a rectangular slit having two layers of equidistant and parallel cylindrical filaments with a diameter of half of the channel height. This spacer geometry is commonly characterised by the ratio of the distance between consecutive filaments to the channel height (L/h), the angle between crossing filaments (β), and the flow attack angle (α) (please see Fig. 1). Values considered in this work were, respectively, 3, 90° and 0° . The flow is assumed to be periodic in each cell, therefore the computational domain is formed by four neighboring spacer filaments as shown in Fig. 1.

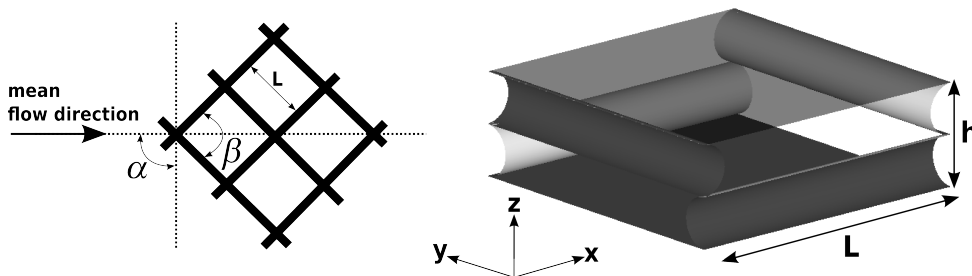


Figure 1: Geometric characterisation of a spacer

The governing equations for a periodic and unsteady flow of a Newtonian fluid are comprised by the mass continuity and Navier–Stokes equations, which are given by:

$$\nabla \cdot \mathbf{U} = 0 \quad (1)$$

$$\frac{\partial \mathbf{U}}{\partial t} + \nabla \cdot (\mathbf{U}\mathbf{U}) - \nabla \cdot \nu \nabla \mathbf{U} = -\nabla p^* \quad (2)$$

where \mathbf{U} is the velocity, ν is the kinematic viscosity, and p^* is a periodic kinematic pressure that includes a pressure gradient increment computed in each iteration necessary to maintain a prescribed mass flow rate.

The periodic solute mass fraction field is determined after calculation of the velocity and pressure fields as:

$$\frac{\partial \omega_A^*}{\partial t} + \nabla \cdot (\mathbf{U}\omega_A^*) - \nabla \cdot D_{AB} \nabla \omega_A^* = S_A \quad (3)$$

where S_A is a source term related to an artificial production of mass in the computational domain necessary to avoid solute mass fraction depletion due to mass transfer at the walls. The S_A source term is given by:

$$S_A = \frac{-D_{AB}}{V} \left(\sum_i S_{f,i} \left(\frac{\partial \omega_A^*}{\partial z} \right) \Big|_{\text{wall}_1} + \sum_i S_{f,i} \left(\frac{\partial \omega_A^*}{\partial z} \right) \Big|_{\text{wall}_2} \right) \quad (4)$$

where $S_{f,i}$ is the area of the i^{th} wall patch face, V is the total volume of the computational domain and z is the direction normal to each wall where mass transfer takes place.

The mass transfer performance of the spacer is commonly determined through the calculation of the local Sherwood number in the membranes by:

$$\text{Sh} = \frac{k_c h}{D_{AB}} \quad (5)$$

where D_{AB} is the solute diffusivity, and k_c is the mass transfer coefficient given by:

$$k_c = \frac{-D_{AB} \left(\frac{\partial \omega_A^*}{\partial z} \right) \Big|_{\text{wall}}}{\omega_{A,\text{bulk}}^* - \omega_{A,\text{wall}}^*} \quad (6)$$

Cyclic boundary conditions were applied in order to cope with flow and mass transfer periodicity in the computational domain. Dissolving wall boundary conditions were defined for the upper and lower walls through the specification of a constant solute mass fraction at the wall ($\omega_A^* = 0$).

3 NUMERICAL METHOD

The computational mesh shown in Fig. 2 was generated using OpenFOAM's blockMesh, transformPoints, mergeMeshes and stitchMesh utilities. A block-structured mesh was developed initially for the lower section of the computational domain. Then, this mesh was replicated, rotated and translated in order to obtain the upper section of the domain. Finally, both meshes were merged with mergeMeshes, and the internal patches resulting

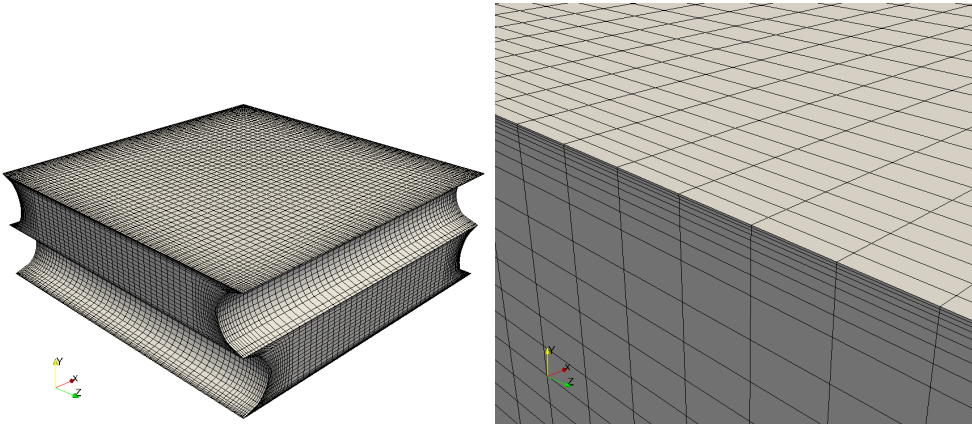


Figure 2: Computational mesh

from the merge were removed with `stitchMesh`. The mesh comprised blocks of $100\ \mu\text{m}$ near both mass transfer boundaries in order to adequately capture the concentration boundary layers (please see Fig. 2, right). The cell layers in those blocks expanded smoothly from the wall with an expansion ratio in the range from 1.1 to 1.5.

The finite-volume solver used for the solution of the Navier-Stokes equation and solute continuity was developed with the OpenFOAM 1.6 distribution, using the `channelFoam` solver as a template. The PISO loop in `channelFoam` was replaced by PIMPLE to better control the convergence stability of the solver, and the solute mass fraction equation and Sherwood number calculation were introduced after the PIMPLE loop. The convection terms were discretized with the `limitedLinear` scheme, while the backward scheme was chosen for the transient terms. The GAMG linear solver was used in this work for all variables, and two inner-loop correctors in the PIMPLE algorithm were found to be sufficient. The number of outer-loop correctors was varied between 2 and 4, depending on the mesh density and Re . Under-relaxation coefficients of 0.3 and 0.7 were used for pressure and velocity, respectively. The transport equations were solved without turbulence modelling for Reynolds numbers of 100 and 200 (based on the channel height), typical of industrial applications, and Schmidt numbers in the range from 1 to 6000. At these Re the flow is expected to be unsteady², so in each simulation the governing equations were integrated in time until obtaining a statistically steady state in terms of area-averaged wall shear stress and Sherwood number. The computations were ran in parallel on a 254 CPU's Linux cluster (openSUSE 11.1 64 bits, Sun Grid Engine), where the meshes were decomposed with a ratio of 100 k cells/CPU using the Scotch decomposition method. The computational time-step was automatically adjusted during run time in order to maintain a Courant number below unity. The time-step was found to vary between 0.01 ms and 0.1 ms, depending on the Re and mesh density.

4 RESULTS

4.1 Velocity patterns

Figure 4 shows some of the flow features from the computational results in terms of time-averaged velocity field for a Re of 200. It should be mentioned that these results compare very well with those obtained by Koutsou et al.² using a commercial CFD package (Fluent). Streamlines in the center of the flow cell disclose a large vortex along its diagonal, which may be regarded as its primary flow feature. Time-averaged local wall shear stress values and their fluctuations in the upper and lower walls are shown in Fig. 5. It may be observed that these fields present symmetric patterns with respect to the channel diagonal, which can be attributed to the symmetric properties of the computational domain. Both wall shear stress magnitude and its fluctuations are higher in the regions close to the inlets and outlets of the domain, where the fluid accelerates due to constricted flow path. The lower values are found in the regions in-between the filaments and the upper and lower walls.

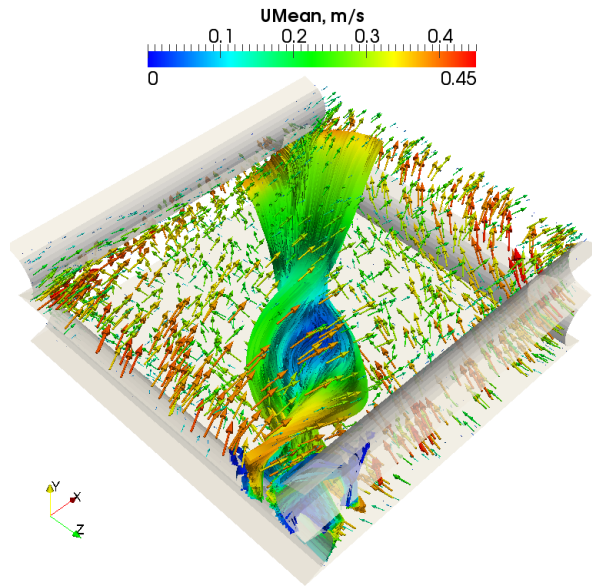


Figure 3: Vectors and streamlines of time-averaged velocity

4.2 Sherwood number patterns

As shown in a previous work¹, wall shear stress can be directly linked to mass transfer in spacer-filled channels. The patterns of time-averaged Sh magnitude and its fluctuations in the upper and lower walls are presented in Fig. 6 for a Re of 200 and a Sc of 6000. A very similar pattern to that of wall shear stress in Fig. 5 can be observed, which further supports the very important effect of wall shear stress on mass transfer.

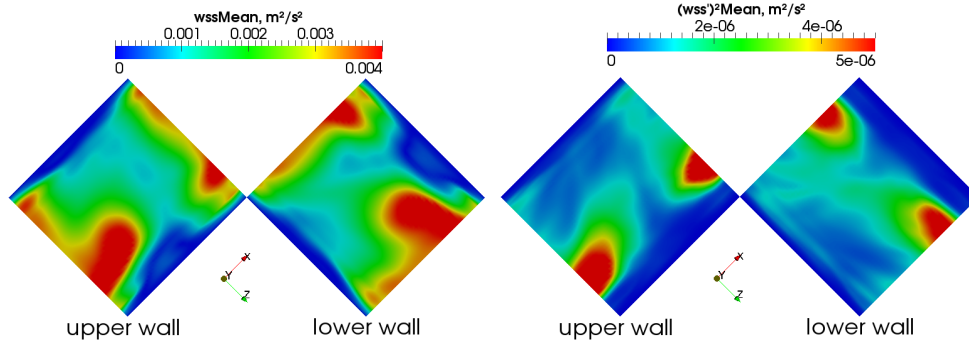


Figure 4: Local time-averaged wall shear stress magnitude and fluctuations

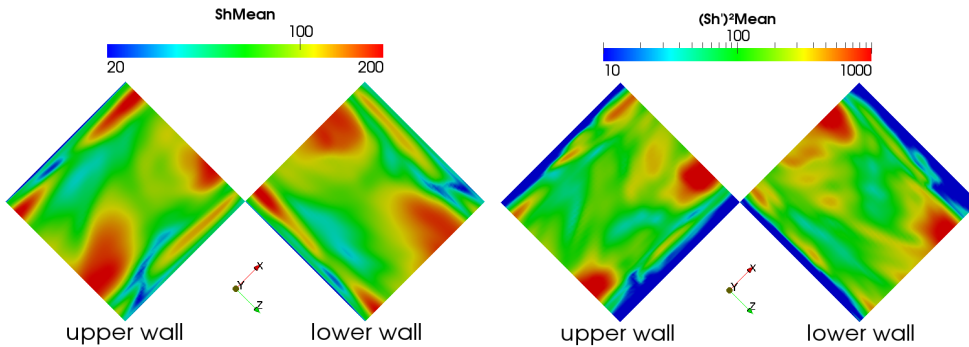


Figure 5: Local time-averaged Sherwood and fluctuations

4.3 Mass transfer correlation

The computational results obtained were used to build quantitative engineering correlations in the form of $Sh = aRe^bSc^c$. Figure 7 compiles the results obtained for Re 100 and 200, and for Sc in the range from 1 to 6000. The best fit results are shown as a dashed line in Fig. 7, and indicate an exponent of 0.52 for Re and 0.31 for Sc . These results are in contradiction with those obtained recently by Koutsou et al.², where values of 0.62 and 0.38 were determined for the exponents of Re and Sc . It should be stressed however that Koutsou et al. performed mass transfer simulations in the Sc range from 1 to 100, whereas this work extended the range of Sc to 6000.

5 CONCLUSIONS

Flow and mass transfer in a spacer-filled channel was studied using OpenFOAM. A particular focus was given to systems exhibiting high Schmidt numbers. It was found that the numerical methodology followed in this work provided similar flow patterns than those found in the literature, while extending the range of Sc numbers commonly investigated to 6000. The Re and Sc dependence of the mass transfer correlation developed from the numerical results is in contradiction to a recent publication by Koutsou et al. [2]. The reasons behind such deviation should be clarified through validation with experimental

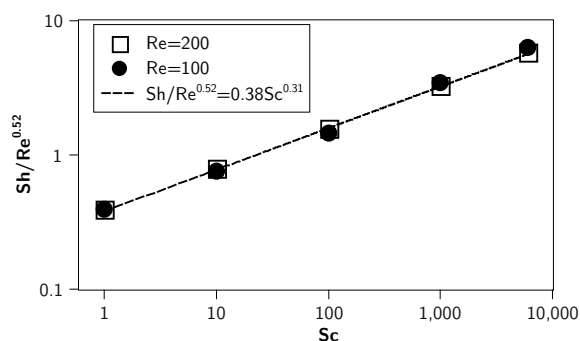


Figure 6: Mass transfer correlation determined by CFD

results.

ACKNOWLEDGEMENTS

The author Vítor Geraldes is grateful to Fundação para a Ciência e a Tecnologia for the financial support through the project PTDC/EQU-EQU/65920/2006.

REFERENCES

- [1] J.L.C. Santos, V. Geraldes, S. Velizarov and J.G. Crespo, Investigation of flow patterns and mass transfer in membrane module channels filled with flow-aligned spacers using Computational Fluid Dynamics (CFD), *Journal of Membrane Science* **305**, 103–117 (2007).
- [2] C.P. Koutsou, S.G. Yiantsios, A.J. Karabelas, A numerical and experimental study of mass transfer in spacer-filled channels: Effects of spacer geometrical characteristics and Schmidt number, *Journal of Membrane Science* **326**, 234–251 (2009).
- [3] G.A. Fimbres-Weihs, D.E. Wiley, Review of 3D CFD modeling of flow and mass transfer in narrow spacer-filled channels in membrane modules, *Chemical Engineering and Processing: Process Intensification*, article in press, doi:10.1016/j.cep.2010.01.007 (2010)